JACS
JOURNAL OF THE AMERICAN CHEMICAL SOCIETY

ARTICLE

pubs.acs.org/JACS

Preparation and Properties of Vesicles Made of Nonpolar/Polar/Nonpolar Fullerene Amphiphiles

Tatsuya Homma,[†] Koji Harano,[†] Hiroyuki Isobe,[‡] and Eiichi Nakamura*[,†]

[†]Department of Chemistry, The University of Tokyo, Hongo, Bunkyo-ku, Tokyo 113-0033, Japan

[‡]Department of Chemistry, Tohoku University, Aoba-ku, Sendai 980-8578, Japan

Supporting Information

ABSTRACT: Twenty potassium complexes of penta-[(4-substituted)phenyl][60]fullerene anions were synthesized and examined for their ability to form bilayer vesicles in water. The 4-substituents include alkyl groups ranging from methyl to icosanyl groups and perfluoromethyl, perfluorobutyl, and perfluorooctyl groups. The overall structure of the amphiphiles can be described as a nonpolar/polar/nonpolar (n−p−n′) motif as opposed to the usual polar/nonpolar motif of lipid amphiphiles. Despite the hydrophobicity of the fullerene moiety (n-part) and alkyl/perfluoroalkyl chains (n′-part), all compounds except for the one with perfluoromethyl groups were soluble in water because of the centrally located fullerene cyclopentadienide (p-part) and spontaneously formed a vesicle of 25- to 60-nm diameter with a narrow unimodal size distribution. The vesicles are stable upon heating to 90 °C or standing over one year in air, as well as on a solid substrate in air or in vacuum, maintaining their spherical form. The vesicle membrane consists of an interdigitated bilayer of the amphiphile molecules, in which the fullerene n-part is inside and the n′-side is exposed to water. These vesicles, in particular the one bearing icosanyl chains, exhibit the smallest water permeability coefficient ever found for a self-assembled membrane in water.

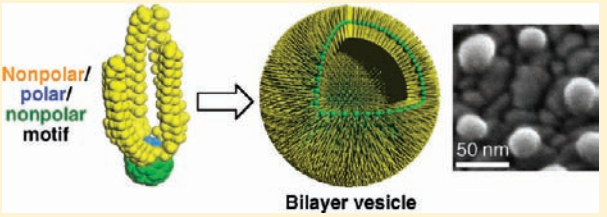

Polar head/nonpolar tail is the archetypal structural motif of lipids that plays crucial roles in the formation of compartment structures both in biology[1] and in man-made systems.[2] In water, the polar heads of the lipid molecule align toward the aqueous environment, while the tails cluster together to form a bilayer membrane. The polymorphic behavior of lipid amphiphiles is a typical characteristic of the lipid bilayer and endows the bilayer with properties characteristic of cell membranes such as mechanical stability and water permeability.[3] The question arises of whether the polar head/nonpolar tail motif is the only motif of the molecules that form a bilayer membrane in water. We made a discovery some time ago that a fullerene anion bearing five phenyl groups on the top side of the molecule (**PhK**, Figure 1a) in water spontaneously forms a bilayer vesicle that shows a unimodal distribution with a diameter centering at ca. 30 nm[4] and exhibits extremely low water permeability (Figure 1c and 1d).[5] Although the structure is quite unusual, **PhK** still has a polar/nonpolar motif (Figure 1b), and the cyclopentadienyl anion and the phenyl groups are exposed to the vesicle surface (Figure 1c and d). With this vesicle structure in mind, we asked whether we could install a hydrophobic chain on each phenyl group (cf. Figure 1e) to create a nonpolar/polar/nonpolar (n−p−n′) motif, and whether such a molecule would still form a bilayer vesicle in water. We previously communicated[6] a remarkable observation that this type of anion, a fullerene anion bearing five perfluorooctyl chains **Rf8K** (Figure 1a), indeed forms a vesicle and that its surface is covered by fluorous chains.

We report in this article that the n−p−n′ motif of the amphiphile is very general, as examined for 18 new fullerene anions bearing methyl to icosanyl, perfluoromethyl, and perfluorobutyl chains (compounds **C1K**−**C13K**, **^{i}C3K**, **^{t}C4K**, **C20K**, **Rf1K**, and **Rf4K**, respectively). All compounds except **Rf1K** formed vesicles with a diameter of 20−60 nm simply by injection of their THF solution into water, and the vesicles exhibited a variety of properties that are unknown for lipid vesicles. For instance, the size distribution of the vesicle is unimodal without any purification, and water permeation through the vesicle membrane is exceedingly slow. Spin coating of the vesicle solution on a hydrophilic solid substrate of mica and indium tin oxide (ITO) dispersed the spherical vesicle particles uniformly on the surface with retention of the spherical shape, in contrast to lipid vesicles.[1] All available evidence indicates that the interdigitated bilayer in the n−p−n′ fullerene vesicle is a hard shell rather than a flexible membrane.

RESULTS AND DISCUSSION

Synthesis of Fullerene Derivatives and Vesicle Formation in Water. The protio fullerene compounds (**CnH** and **RfnH**) were synthesized by 5-fold addition of a 4-substituted phenylcopper reagent to [60]fullerene (58−99%) as shown in

Received: January 18, 2011
Published: April 01, 2011

dx.doi.org/10.1021/ja200498g | J. Am. Chem. Soc. 2011, 133, 6364–6370

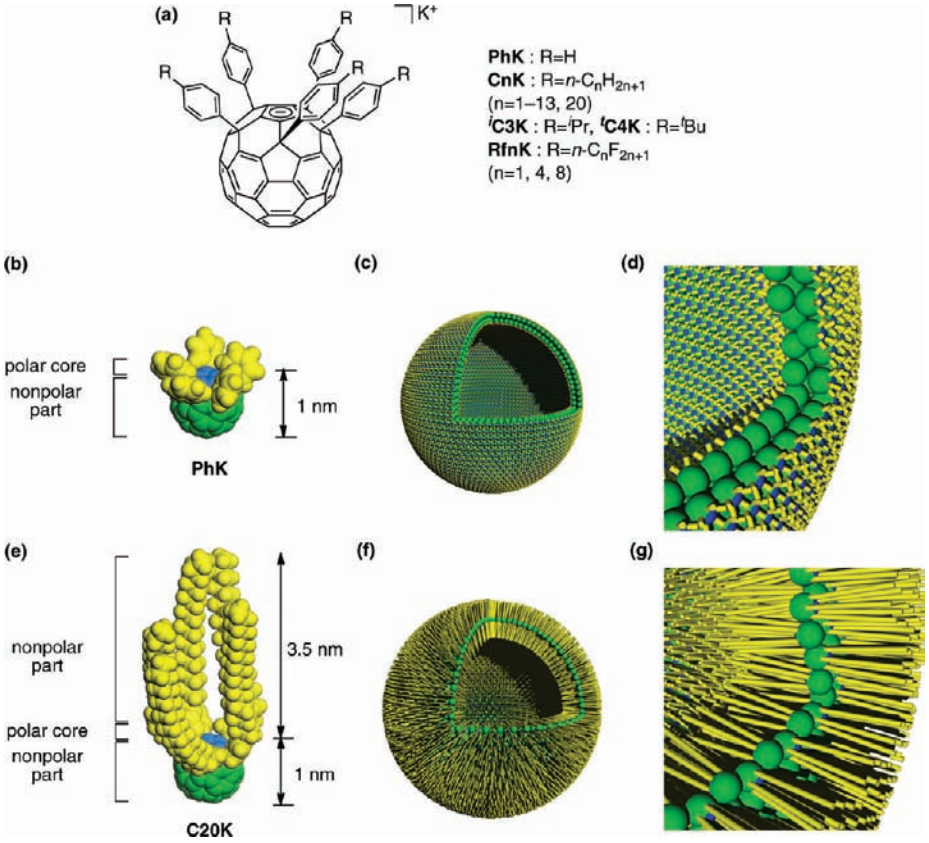

Figure 1. Schematic images of vesicles made of fullerene anions. (a) Chemical structures of potassium complexes of fullerene anions. (b) CPK drawing of **PhK**. (c) Schematic model of bilayer vesicle of **PhK**. (d) A magnified image of the bilayer **PhK** vesicle. (e) CPK drawing of **C20K**. (f) Schematic model of a vesicle of **C20K**. (g) A magnified image of the interdigitated bilayer of the **C20K** vesicle. The fullerene parts are shown in green, the hydrophilic parts in blue, and substituents in yellow.

Scheme 1. Preparation of Fullerene Vesicles

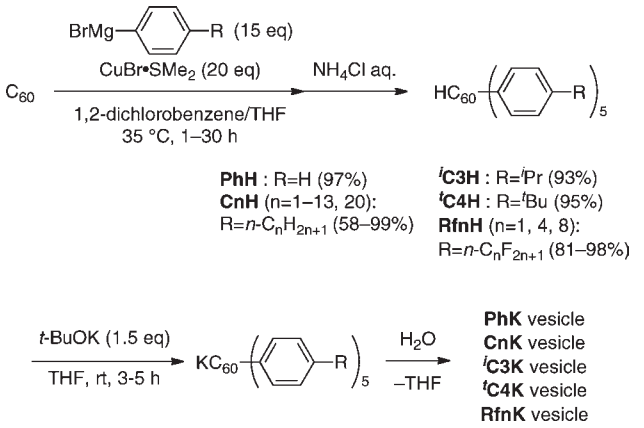

Scheme 1.[7] They were treated with *t*-BuOK in THF to form a homogeneous solution of **CnK** and **RfnK**, which was injected into water (followed by removal of THF under reduced pressure) to form a homogeneous vesicle solution of the potassio fullerene. The vesicle solution thus prepared is orange, homogeneous, clear without any purification, and stable for over a year under air on a shelf.

The protio and the potassio fullerenes behave very differently from each other. **Rf8H** and **Rf8K** are illustrative of this fact. The

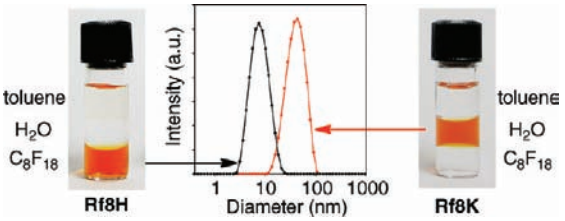

Figure 2. A solution of fullerene pentaadduct and the corresponding potassium salt in a triphase system of toluene (top phase), water (middle phase), and C_8F_{18} (bottom phase) and the size distribution determined by DLS (carried out in pure solvent). **PhH** dissolves in toluene, **Rf8K** dissolves in water, and **Rf8H** dissolves in C_8F_{18} but only sparingly in toluene.

protio compound **Rf8H** is insoluble in water, sparingly soluble in toluene, and soluble in perfluorooctane (C_8F_{18}) as an aggregate with a diameter of 8.1 nm as determined by dynamic light scattering (DLS; Figure 2), perhaps micelles that expose the fluorous chain on the outer surface. In contrast, the potassio compound **Rf8K** dissolved in THF as a monomer (ca. 1 nm in diameter by DLS), suggesting that the solubility in THF is gained by formation of a solvent-separated ion pair, as was found previously in the crystal structure of **PhK**.[8] The potassium complex **Rf8K** dissolves quite well in water (up to 10 g/L at 25 °C) to form an orange solution of vesicles with a diameter of 36.2 nm (Figure 2). Notably, the lithium and sodium complexes

dx.doi.org/10.1021/ja200498g |*J. Am. Chem. Soc.* 2011, 133, 6364–6370

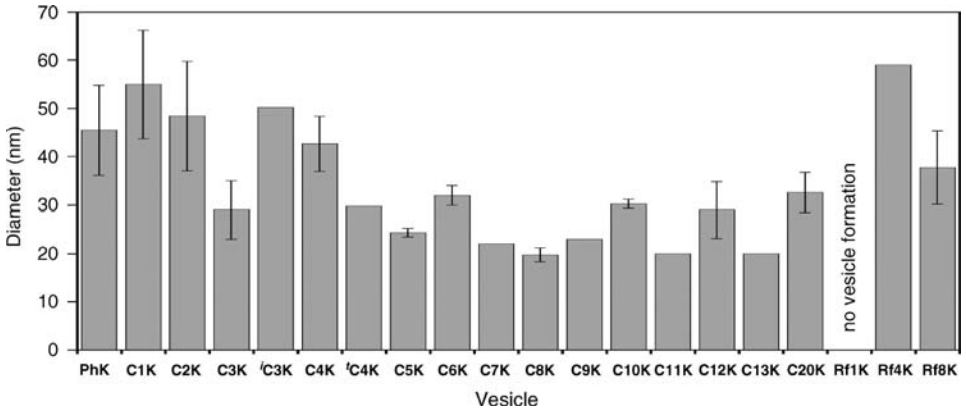

Figure 3. Diameter of fullerene vesicles in water determined by DLS measurement at 25 °C. The data with error bars were determined by at least three vesicle preparations. The data for **PhK** and **Rf8K** agree with the values reported in refs 4 and 6.

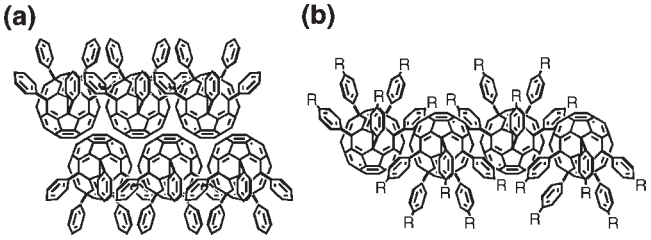

Figure 4. Schematic illustrations of two membrane structures. (a) Archetypal bilayer where the area per one fullerene molecule is about 0.6 nm^2 and (b) an interdigitated bilayer where the area is approximately twice as large.

precipitated in water, indicating that the potassium cation is responsible for the high solubility of **Rf8K** in water. **Rf4K** behaves similarly to **Rf8K**, but the vesicle of **Rf1K** is unstable and precipitates in water and hence was not examined further.

The 16 alkylphenyl compounds **CnK** dissolve well in water, like **Rf4K** and **Rf8K**, to form a vesicle solution of up to 2−4 mM concentration. However, the solubility of the protio compounds **CnH** depended markedly on the alkyl group. For instance, **C20H** dissolves well both in toluene and in hexane, whereas **PhH** dissolves in toluene but not in hexane.

Laser Light Scattering (LLS) Studies of Fullerene Vesicles in Water. The 19 vesicle-forming potassium complexes (**PhK**, **CnK**, **Rf4K**, and **Rf8K**) showed a unimodal diameter distribution ranging between 20 and 60 nm as judged by DLS (Figure 3). The vesicle size was found not to change much after one year on a shelf or over 1 h at 90 °C. Zeta potentials are negative (−30 to −50 mV), which suggests that the vesicle exists as a solvent-separated ion pair in water.

To determine the structure of the vesicle further, we analyzed the **Rf8K** vesicle by static light scattering (SLS). For a solution that gave us a hydrodynamic radius (R_h; by DLS) of 26.7 nm, the SLS analysis gave us a radius of gyration (R_g) of 26.7 nm. The R_g/R_h ratio being 1.00, we conclude that the vesicle is hollow.[9] The Zimm square plot gave a molecular weight of 1.94×10^7 Da, indicating that a vesicle contains 5.98×10^3 molecules of **Rf8K**. From this number and the surface area of a vesicle, we obtain an area of 1.39 nm^2/molecule, which is twice as large as the 0.59 nm^2/molecule area of the **PhK** vesicle (an archetypal bilayer shown in Figures 4a and 1d).[4b] We consider that **Rf8K** forms an interdigitated bilayer (Figures 4b and 1g) on the basis of the

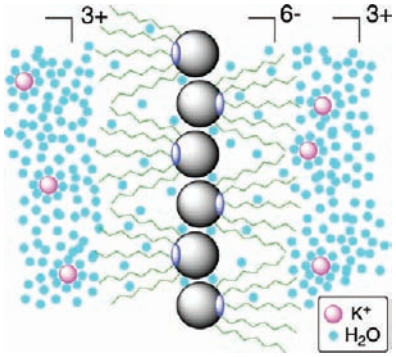

Figure 5. Schematic model of the bilayer showing a solvent-separated ion-pair structure. Alkyl- or perfluoroalkyl-substituted fullerenes in gray, potassium cation in pink separated from the cyclopentadienide anion on fullerene in blue, and water in light blue.

1.22 nm^2/molecule area found in the crystal of a structurally similar penta-4[(trimethylsilyl)ethynylphenyl]fullerene compound.[10,11]

We consider that the potassium cation located in the aqueous phase endows water solubility to the vesicles as illustrated in Figure 5 on the basis of the following experimental results. The first is the negative zeta potentials of the vesicle surface, suggesting that the amphiphile exists as a solvent-separated ion pair. Second, the reported crystal structures of **PhK** indicated that the bulky five phenyl groups force the bulky potassium ion away from the fullerene's anion center, prevents the formation of a contact ion pair, and consequently creates a solvent-separated ion pair.[8] The fact that lithium and sodium analogs of **PhK** do not dissolve in water suggests that these metals form a contact ion pair and do not contribute to the increase of the water solubility.

NMR Studies of Fullerene Vesicles in Water. Neither the **C8K** nor the **Rf8K** vesicle in D_2O exhibited any signals in the ^1H, ^{13}C, or ^{19}F NMR spectra at 25 and 80 °C. On the other hand, the ^1H NMR spectra of the **C20K** vesicle showed no signals below 40 °C but suddenly showed, at 50 °C or higher, the terminal CH_3 and CH_2 signals (Figure 6), a behavior suggesting the melting of the alkyl chains. This behavior is entirely different from that of lipid molecules in a bilayer membrane, where the alkyl chains give ^1H NMR signals at room temperature because they are mobile.[12] The CH_2/CH_3 signal ratio changed from 24:3 (50 °C), 30:3 (60 °C), to 32:3 (70 °C) (Figure S3). Thus, the terminal groups are more mobile than the internal CH_2

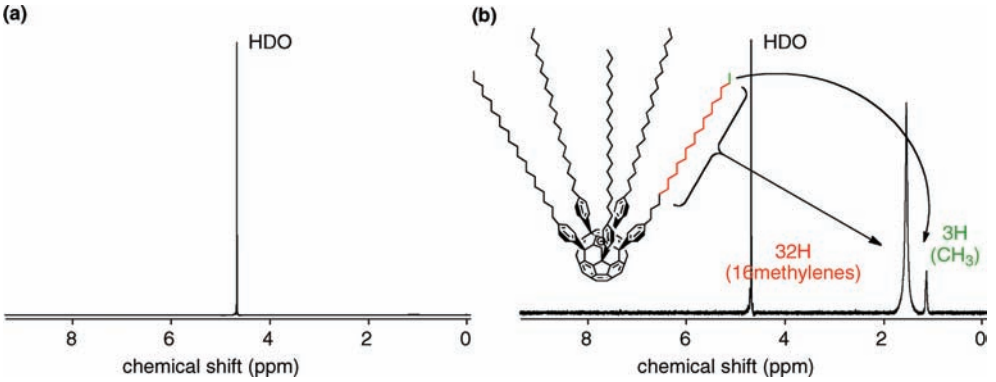

Figure 6. ^{1}H NMR spectra of **C20K** vesicle in D_2O at (a) 20 and (b) 70 °C.

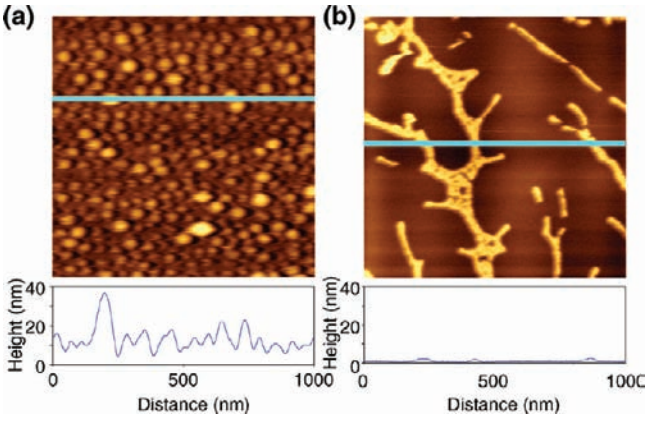

Figure 7. AFM images of the HOPG surface after drop-casting of a 2 mM solution of **C20K** and **PhK**. The cross-section profiles along the light-blue line in each figure are shown below the AFM images. (a) The HOPG surface covered by **C20K** vesicles. Note that the diameter of the vesicle in the lateral direction is greatly overestimated because of the intrinsic limitations of AFM. (b) The HOPG surface after drop-casting of **PhK**, where we could not identify any vesicular objects and instead found ill-defined objects with 1- to 2-nm heights.

groups, which agrees with our proposal that alkyl groups are exposed to the aqueous phase.

Microscopic Studies of Fullerene Vesicles on Highly Oriented Pyrolytic Graphite (HOPG), Mica, and ITO. Microscopic studies of the fullerene vesicles on a solid surface revealed that these vesicles are nearly perfectly spherical and are robust enough to retain their shape in air or in vacuum. This behavior is entirely unknown for lipid vesicles, which are flexible and lose their structural integrity upon drying or in vacuum.

When we drop-cast the **C20K** vesicle on HOPG and examined it by atomic force microscopy (AFM) under air, we saw uniformly dispersed spherical particles having a height of 20 to 30 nm (Figure 7a). The height agrees well with the diameter determined by DLS. Interestingly, the **C20K** vesicles on HOPG formed a uniform monolayer without forming domains or multilayers while the **PhK** vesicle showed ill-defined objects with 1- to 2-nm heights (Figure 7b). We ascribe the latter observation to the decomposition of the vesicle structure because of the more favorable interaction of the fullerene part of the **PhK** molecule with HOPG than the hydrophilic cyclopentadienide part that was exposed to the aqueous phase before HOPG is coated (Figure 8).

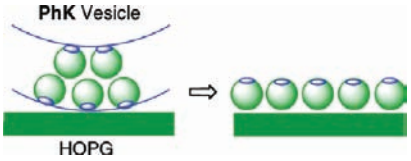

Figure 8. Illustration of decomposition of the **PhK** vesicle on HOPG. Green balls represent the fullerene core, and the blue region represents the hydrophilic cyclopentadienide part.

When drop-cast on mica, the vesicles of **PhK**, **CnK** (n = 4, 8, 12, 20; 2 mM as for the fullerene molecule), and **Rf8K** retained their spherical shape and became uniformly dispersed without the formation of domains or islands. The density of the vesicles was found to be rather uniform: 63, 80, 75, 100, 85, and 60 vesicles/μm^2, respectively (see Supporting Information).

High-resolution SEM analysis of the **Rf8K** vesicle on a semiconducting ITO surface afforded an interesting piece of information on the manner in which the vesicles interact with the solid substrate. The low-magnification top view in Figure 9a shows that the vesicle particles uniformly cover a wide area of the ITO substrate. A closer look (Figure 9b) reveals that the vesicles sit on the grain boundaries of the ITO surface to maximize contact with the surface. The 30°-tilted side view (Figure 9c) not only confirms this observation but also indicates that the vesicles largely retain their spherical structures under the rather harsh SEM conditions of 10^{-5} Pa, which attests to the unusual robustness of the fullerene vesicle. The average diameter of the **Rf8K** vesicle particles was found to be 35.6 $\pm$ 0.4 nm as measured for 190 vesicles (Figure 9a), which matched very well with the DLS diameter (36.2 $\pm$ 0.2 nm, Figure 2).[6]

It is interesting to note that we could not fill the ITO grain boundary completely with the vesicle particles (94% of the 545 particles are separated from each other) and the surface coverage remained at the rather constant value of 228 $\pm$ 14 particles/μm^2 as examined under two independently prepared samples by spin coating of a 2 mM **Rf8K** solution. Possibly, the vesicle particles recognize some very special structures of the grain boundary.

Contact Angle of Water on Vesicle-Coated Mica and Soda-Lime Glass Surfaces. The coverage of the hydrophilic surface of mica and soda-lime glass with the hydrophobic vesicles was found to make the surface water-repellent, as examined for the vesicles of **PhK**, **CnK** (n = 4, 8, 12, 20), and **Rf8K**.

As summarized in Figure 10 for mica (blue) and glass (red), the contact angle properties may be classified into three classes,

dx.doi.org/10.1021/ja200498g |*J. Am. Chem. Soc.* 2011, 133, 6364–6370

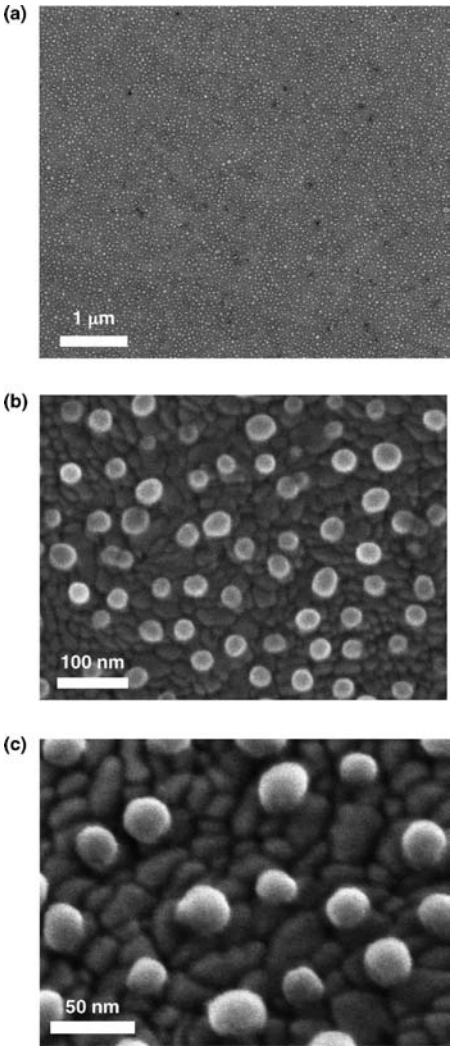

Figure 9. SEM images of **Rf8K** vesicles on ITO under ca. 10^{-5} Pa. (a) SEM image of **Rf8K** vesicles on the ITO surface. (b) Magnified view of Figure 9a. (c) A different area of the same sample as viewed with a 30° tilt of the sample stage.

PhK, **CnK**, and **RfnK**. For the **CnK** vesicles, the contact angle on mica for the alkyl substituted fullerenes increased as the hydrophobicity (alkyl chain length) increased: **C4K** (14.2 ± 2.0)° < **C8K** (27.3 ± 4.1)° < **C12K** (52.0 ± 4.2)° < **C20K** (85.9 ± 3.6)°. Once the surface was dried, the surface remained water-repellent even after repeated rinsing with water and after storage in air at room temperature for several months. The behavior of the **PhK** vesicle is similar to that of **C8K**, while that of **Rf8K** is similar to that of **C20K**. We surmise that the drying changed the surface structure of the vesicle. One possibility would be that dehydration of the potassium cation pushed the metal atom from the surface of the vesicle into the membrane interior.

Water Permeability of Fullerene Vesicles. Water permeation is one of the fundamental properties of lipid and surfactant membranes,[1,3,12] and hence those of the **C4K**, **C8K**, **C12K**, **C20K**, and **Rf8K** vesicles were studied by the ^{17}O NMR method reported for the **PhK** vesicle.[5,13]

The **PhK** vesicle exhibits unusual kinetics and very low water permeability.[5] The permeation constant P is 3 orders of magnitude smaller than known values for lipid vesicles. The very slow water permeation is due to a very large negative entropy barrier that has been ascribed to the capture of gaseous water molecules by fullerenes,[14] accompanied by a large negative activation enthalpy (Figure 11c, leftmost column). Note that the barrier for water permeation through a lipid membrane is due to a positive activation enthalpy (a barrier for water gasification).[1,3,15] In addition, the permeability peaks at ca. 40 °C and decreases toward 80 °C where the vesicle still maintains its structural integrity (see Figure 11a, blue line bending at ca. 40 °C). This may be ascribed to a phase transition characteristic of fullerene derivatives in the solid state, as found for some fullerene derivatives.[16]

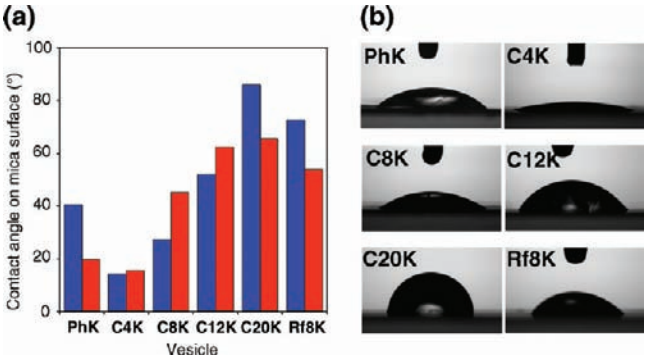

Figure 10. (a) Contact angles of water on a vesicle-coated mica surface (blue) and a vesicle-coated glass surface (red). (b) Photographs of water droplet (3 μL) on vesicle-coated mica surface.

Comparison of the permeability properties of the **PhK** vesicle with those of the **C4K**, **C8K**, **C12K**, **C20K**, and **Rf8K** vesicles first indicated that the **C4K** vesicle is several times more leaky than the **PhK** vesicle and the permeability decreases as the alkyl chain becomes longer or perfluorooctyl groups are introduced (Figure 11b). To our knowledge, the permeation constant of $P = (1.69 \pm 0.10) \times 10^{-7}$ m/s is the smallest value reported for a self-assembled membrane.[2b] It is reasonable to assume that the membrane becomes leaky because of the steric bulk of the *p*-alkylphenyl groups (i.e., n′-group), which loosens the molecular packing (see above for the increase in the area occupancy per molecule as it goes from **PhK** to **Rf8K**, and the likely change of the molecular packing as illustrated in Figure 4), but becomes less leaky as the hydrophobicity of the n′-group becomes larger as the chain becomes longer. We consider that the low water permeability of **C20K** is due to the hydrophobic effects of the long alkyl chains and the enhanced stability of the membrane caused by the intermolcular van der Waals interactions. Interestingly, the permeability constant P in Figure 11b is inversely related to the magnitude of the contact angle shown in Figure 10. It is possible that the contact angle reflects the properties of the fullerene bilayer, because the contact angle has been reported to reflect the properties of a self-assembled monolayer up to a depth of about 2 nm.[17]

The permeability curve (Figure 11a) peaks at ca. 40 °C for the **PhK** and **C4K** vesicles, at 30 °C for **Rf8K**, and at 20 °C or below for **C8K**, and no peak appears for **C20K**. This trend agrees with the profile of activation enthalpy and entropy, where both parameters become less sensitive as the chain becomes longer from C12 to C20 (Figure 11c). We surmise that the fullerene part determines the profile of water permeability in the **PhK** vesicle while the hydrophobicity of the alkyl chains contributes to the

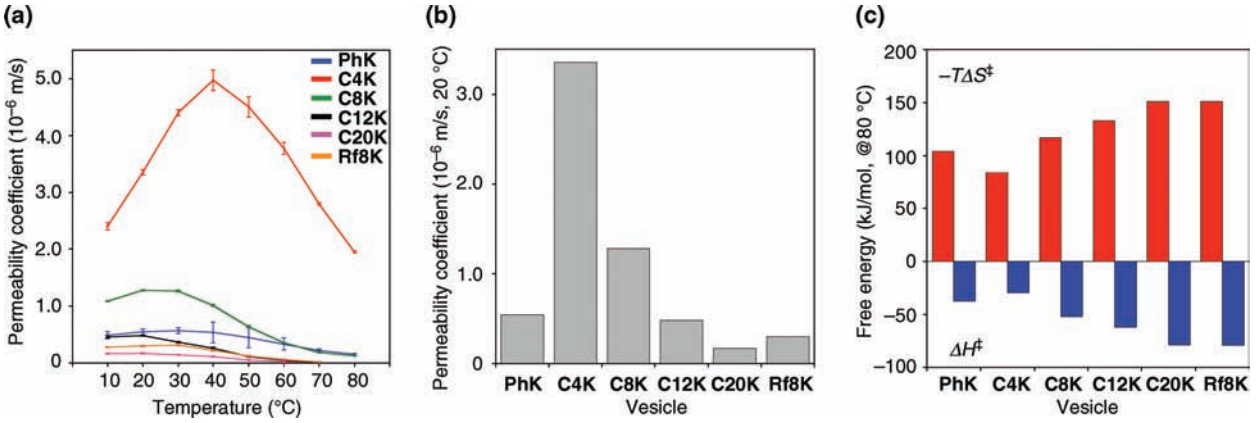

Figure 11. Water permeation through fullerene membranes. (a) Temperature dependence of water permeability of fullerene vesicles **PhK**, **C4K**, **C8K**, **C12K**, **C20K**, and **Rf8K**. Error bars show the standard errors of the mean of three measurements. (b) Permeability coefficients of water through fullerene membranes measured at 20 °C. Permeability coefficients at 20 °C: **PhK**: $P = (5.45 \pm 0.32) \times 10^{-7}$ m/s, **C4K**: $P = (3.36 \pm 0.05) \times 10^{-6}$ m/s, **C8K**: $P = (1.28 \pm 0.01) \times 10^{-6}$ m/s, **C12K**: $P = (4.82 \pm 0.12) \times 10^{-7}$ m/s, **C20K**: $P = (1.69 \pm 0.10) \times 10^{-7}$ m/s, **Rf8K**: $P = (3.01 \pm 0.09) \times 10^{-7}$ m/s. (c) Activation enthalpy ($\Delta H^{\ddagger}$) and activation entropy ($-T\Delta S^{\ddagger}$) values for water permeation at 80 °C. Data for the **PhK** vesicle are cited from ref 5.

decrease of the permeability in the **C20K** vesicle (and the **Rf8K** vesicle).

CONCLUSION

We have studied the behavior of 20 fullerene anions, **PhK**, **C1K**−**C20K**, **^{i}C3K**, **^{t}C4K**, **Rf4K**, and **Rf8K**, and found that the fullerene anions having a nonpolar/polar/nonpolar (n−p−n′) motif spontaneously form an interdigitated bilayer vesicle in water. All vesicles obtained in this study show essentially the same physical properties despite the diversity of the substituents. The SEM and AFM images indicate that the vesicles are spherical and very robust, indicating that the vesicle is more like an eggshell than a biological cell. This robustness is one reason for the low water permeability.

The exposure of the hydrophobic groups to the aqueous environment that we propose is supported by several experiments. First, VT NMR experiments indicated the higher mobility of terminal CH_3 groups compared to the internal CH_2 groups in the **C20K** vesicle (Figure 6). Second is the observed systematic dependency of the water contact angle on the alkyl chains (Figure 10). The third is the fact that both **PhK** and **C20K** show similar temperature dependence profiles of water permeation, which is different from those reported for lipid vesicles (Figure 11a). Finally, it is known that the fullerene/fullerene cohesive power is extremely high (much higher than the hydrocarbon/hydrocarbon interaction which is known to be very weak), and it has been demonstrated in many two- and three-dimensional solid states that fullerene molecules stick together very tightly.[18]

One attractive feature of the present vesicle preparation is that we can obtain a morphologically stable, monodispersed, nanometer-size, spherical hollow object by a simple method and without any purification. These n−p−n′-type fullerene anions have little resemblance to lipid molecules, as both ends of the molecule are hydrophobic and the polar anionic part is buried in the molecular structure. The strong cohesive power of fullerene must be instrumental in forming the vesicle assembly. The hydrophobic chains exposed on the surface of the vesicle did not hamper the vesicle formation in water and may have even increased the stability of the vesicles by clustering together on the vesicle surface. The solubility of the molecule appears to be produced by the potassium cation, which is solvated by water molecules and located in the aqueous phase. The n−p−n′ amphiphile provides a hydrophobic surface to a water-soluble hollow object, and this can be achieved by self-assembly. This property suggests applications of the vesicles to the targeted delivery of organic and inorganic materials.[19] In addition, we can envisage the utility of the surface-coating property of the vesicles in the nanolevel surface modification of a solid substrate.[20] These n−p−n′-type amphiphiles will open a new avenue in the research on nanometer-sized compartment structures in solution and on solid surfaces.

ASSOCIATED CONTENT

Supporting Information. Procedures for the synthesis of new compounds; preparation of vesicles; DLS, SLS, AFM, SEM, and water permeability measurements of vesicles; water contact angles of vesicle covered surface; and temperature dependence of ^{1}H NMR of **C20K** vesicle. This material is available free of charge via the Internet at http://pubs.acs.org.

AUTHOR INFORMATION

Corresponding Author
nakamura@chem.s.u-tokyo.ac.jp

ACKNOWLEDGMENT

We thank Mr. K. Murata (FEI Company) for SEM measurements. We thank MEXT (KAKENHI for E.N., No. 22000008, the Global COE Program for Chemistry Innovation, and JSPS predoctoral fellowship for T.H.) for financial support. The generous supply of [60]fullerene from Frontier Carbon Corporation is acknowledged.

REFERENCES

(1) (a) *Vesicles*; Rosoff, M., Ed.; Marcel Dekker: New York, 1996. (b) *Biomembranes*; Gennis, R. B., Ed.; Springer: New York, 1989.

(2) (a) Kunitake, T.; Okahata, Y. *J. Am. Chem. Soc.* **1977**, *99*, 3860–3861. (b) Discher, B. M.; Won, Y. Y.; Ege, D. S.; Lee, J. C. M.;

Bates, F. S.; Discher, D. E.; Hammer, D. A. *Science* **1999**, *284*, 1143–1146. (c) Fuhrhop, J. H.; Bartsch, H. *Liebigs Ann. Chem.* **1983**, *5*, 802–815. (d) Saji, T.; Hoshino, K.; Ishii, Y.; Goto, M. *J. Am. Chem. Soc.* **1991**, *113*, 450–456. (e) Lee, H.-K.; Park, K. M.; Jeon, Y. J.; Kim, D.; Oh, D. H.; Kim, H. S.; Park, C. K.; Kim, K. *J. Am. Chem. Soc.* **2005**, *127*, 5006–5007. (f) Hao, J.; Li, H.; Liu, W.; Hirsch, A. *Chem. Commun.* **2004**, 602–603. (g) Greenfield, M. A.; Palmer, L. C.; Vernizzi, G.; de la Cruz, M. O.; Stupp, S. I. *J. Am. Chem. Soc.* **2009**, *131*, 12030–12031. (h) Babu, S. S.; Möhwald, H.; Nakanishi, T. *Chem. Soc. Rev.* **2010**, *39*, 4021–4035. (i) Versluis, F.; Tomatsu, I.; Kehr, S.; Fregonese, C.; Tepper, A. W. J. W.; Stuart, M. C. A.; Ravoo, B. J.; Koning, R. I.; Kros, A. *J. Am. Chem. Soc.* **2009**, *131*, 13186–13187.

(3) (a) Haines, T. H.; Liebovitch, L. S. *Permeability and Stability of Lipid Bilayers*; CRC: Boca Raton, FL, 1995. (b) Fettiplace, R.; Haydon, D. A. *Physiol. Rev.* **1980**, *60*, 510–550. (c) Reeves, J. P.; Dowben, R. M. *J. Membr. Biol.* **1970**, *3*, 123–141. (d) Sharma, R. R.; Chellam, S. *J. Colloid Interface Sci.* **2006**, *298*, 327–340.

(4) (a) Sawamura, M.; Nagahama, N.; Toganoh, M.; Hackler, U. E.; Isobe, H.; Nakamura, E.; Zhou, S. Q.; Chu, B. *Chem. Lett.* **2000**, *29*, 1098–1099. (b) Zhou, S. Q.; Burger, C.; Chu, B.; Sawamura, M.; Nagahama, N.; Toganoh, M.; Hackler, U. E.; Isobe, H.; Nakamura, E. *Science* **2001**, *291*, 1944–1947.

(5) Isobe, H.; Homma, T.; Nakamura, E. *Proc. Natl. Acad. Sci. U.S.A.* **2007**, *104*, 14895–14898.

(6) Homma, T.; Harano, K.; Isobe, H.; Nakamura, E. *Angew. Chem., Int. Ed.* **2010**, *49*, 1665–1668.

(7) (a) Sawamura, M.; Iikura, H.; Nakamura, E. *J. Am. Chem. Soc.* **1996**, *118*, 12850–12851. (b) Matsuo, Y.; Nakamura, E. *Chem. Rev.* **2008**, *108*, 3016–3028.

(8) Matsuo, Y.; Tahara, H.; Nakamura, E. *Chem. Lett.* **2005**, *34*, 1078–1079.

(9) Burger, C.; Hao, J.; Ying, Q.; Isobe, H.; Sawamura, M.; Nakamura, E.; Chu, B. *J. Colloid Interface Sci.* **2004**, *275*, 632–641.

(10) Zhong, Y. W.; Matsuo, Y.; Nakamura, E. *J. Am. Chem. Soc.* **2007**, *129*, 3052–3053.

(11) The bilayer scheme in Figure 1e in our original Communication (ref 6) needs to be revised.

(12) Shibata, A. *Liposomes in Life Science Experimental Manual*; Terada, H., Yoshimura, T., Eds.; Springer: Tokyo, 1992.

(13) Haran, N.; Shporer, M. *Biochim. Biophys. Acta* **1976**, *426*, 638–646.

(14) Ludwig, R.; Appelhagen, A. *Angew. Chem., Int. Ed.* **2005**, *44*, 811–815.

(15) Zwolinski, B. J.; Eyring, H.; Reese, C. E. *J. Phys. Chem.* **1949**, *53*, 1426–1453.

(16) Matsuo, Y.; Iwashita, A.; Abe, Y.; Li, C.-Z.; Matsuo, K.; Hashiguchi, M.; Nakamura, E. *J. Am. Chem. Soc.* **2008**, *130*, 15429–15436.

(17) Bain, C. D.; Troughton, E. B.; Tao, Y. T.; Evall, J.; Whitesides, G. M.; Nuzzo, R. G. *J. Am. Chem. Soc.* **1989**, *111*, 321–335.

(18) Li, C.-Z.; Matsuo, Y.; Nakamura, E. *J. Am. Chem. Soc.* **2010**, *132*, 15514–15515.

(19) (a) Maeda, R.; Noiri, E.; Isobe, H.; Homma, T.; Tanaka, T.; Negishi, K.; Doi, K.; Fujita, T.; Nakamura, E. *Hypertens. Res.* **2008**, *31*, 141–151. (b) Isobe, H.; Nakanishi, W.; Tomita, N.; Jinno, S.; Okayama, H.; Nakamura, E. *Chem.—Asian J.* **2006**, *1*, 167–175. (c) Maeda-Mamiya, R.; Noiri, E.; Isobe, H.; Nakanishi, W.; Okamoto, K.; Doi, K.; Sugaya, T.; Izumi, T.; Homma, T.; Nakamura, E. *Proc. Natl. Acad. Sci. U.S.A.* **2010**, *107*, 5339–5344. (d) Nakamura, E; Isobe, H. *Chem. Rec.* **2010**, *10*, 260–270.

(20) Katagiri, K.; Hamasaki, R.; Ariga, K.; Kikuchi, J. *J. Am. Chem. Soc.* **2002**, *124*, 7892–7893.